<sup>1</sup>B. Rajapandian <sup>2</sup>G.T. Sundarrajan,

# Analysing Photovoltaic Grid-Connected H5 Inverter with Artificial Intelligence for Induction Motor Load Testing and Evaluation



Abstract: Recent advancements in transformerless photovoltaic (PV) grid-connected inverters have positioned them as a prominent technology for distributed PV power generation systems. This is attributed to their demonstrably superior efficiency, reduced cost, and compact size. Conversely, they are susceptible to common-mode currents, leading to significant electromagnetic interference and security risks, thereby compromising system reliability. We introduced an enhanced H5 variant topology, termed H5-D topology, which integrates a clamping diode to mitigate common-mode voltage fluctuations. The paper presents the simulation results comparing both topology's configurations, with a focus on the H5-D topology's efficiency in suppressing common-mode currents. Additionally, experimental prototypes were constructed and evaluated for both the original and the H5-D configurations topology. The results unequivocally demonstrate the superior performance of the H5-D topology. The experimental findings corroborate the effectiveness of the recommended/suggested topology in addressing current issues related to common-mode issues, thereby enhancing the reliability and performance of photovoltaic inverter systems.

Keywords: Photovoltaic inverters, H5-D topology, Transformerless inverters, Common-mode current, Reliability

#### I. INTRODUCTION

Photovoltaic (PV) energy is widely considered the most attractive and sustainable renewable energy source, available throughout the year. It is anticipated that more than 45% of future power needs will be generated by PV arrays [1]. The cost of PV systems depends largely on the PV module size, making efficient consumption of the electric power they produce crucial for cost reduction. Various system structures can enhance overall system efficiency [2]. Transformerless photovoltaic inverters, that is, grid-connected inveters are increasingly being deployed due to their inherent advantages in size, cost, and efficiency relative to transformer-isolated topologies [3]. However, a significant challenge associated with transformerless inverters is the emergence of common-mode (CM) currents. These currents stem from the parasitic capacitances present between the PV array and ground [2]. The presence of CM currents can introduce several detrimental effects on the system, including electromagnetic interference (EMI), degradation of system reliability, and potential security vulnerabilities, particularly in hybrid energy storage systems that combine PV and battery storage technologies [4]. As a consequence, mitigating CM currents in transformerless PV inverters has become a crucial area of research in recent years. These innovative designs primarily focus on two key strategies: achieving galvanic isolation between the PV array and the grid, or implementing auxiliary clamping circuits to maintain a constant CM voltage within the system [5]. One prominent example is the H5 topology, which introduces a strategically placed switch between the inverter input and the bridge arms, effectively modifying existing configurations to address CM currents [6]. Building upon this concept, the H6 family of topologies employs two additional switches, situated either between the input and bridge arms or directly incorporated within the bridge arms themselves. In contrast, the HERIC family adopts a distinct approach by introducing supplementary freewheeling branches strategically placed between the bridge arms and filter inductors. An alternative strategy for CM current mitigation involves the utilization of clamping circuits to regulate the midpoint voltage of the bridge arms. The neutral-clamp HERIC topology exemplifies this approach by incorporating a dedicated clamping circuit positioned between the midpoint of the input capacitors and the freewheeling branch [7]. For full-bridge inverter configurations, the HB-ZVR topology introduces a novel clamping circuit comprised of a single switch and five strategically placed diodes, positioned between the midpoint of the input capacitors and the bridge arms. Additionally, the split-inductor neutral-point-clamped three-level topology leverages a more traditional approach by incorporating two additional diodes into the conventional full-bridge design [8]. These innovative clamping circuit-based approaches offer effective solutions for mitigating CM currents within transformerless PV inverter systems adjust these margins. Some components, such as multi-leveled

<sup>&</sup>lt;sup>1</sup> Research Scholar, Department of EEE ,Sathyabama Institute of Science and Technology

<sup>&</sup>lt;sup>2</sup>Department of EEE,Sathyabama Institute of Science and Technology

equations, graphics, and tables are not prescribed, although the various table text styles are provided. The formatter will need to create these components, incorporating the applicable criteria that follow.

Transformerless PV grid-connected inverters offer numerous advantages over traditional counterparts, including enhanced efficiency, reduced costs, and compact design. However, the presence of common-mode current poses a significant challenge, leading to electromagnetic interference and security vulnerabilities. This paper investigates the execution of the H5-D topology through simulation and experimental validation, offering insights into its effectiveness in suppressing CM current. Further, the objective of the paper is to (1) Propose an improved H5-D topology for transformerless PV, that is PV grid-connected inverters; (2) Address common-mode voltage fluctuations through the addition of a clamping diode in the H5-D topology; (3) Compare simulation results obtained from both the original H5 and H5-D topology (proposed topology); (4) Analyze the effectiveness of the H5-D topology in suppressing CM current; (5) Construct and test experimental prototypes of both topologies; and (6) Validate the efficiency of the H5-D topology in mitigating CM currents by comparing and analyzing experimental results.

## II. BACK GROUND

Grid-connected PV inverters broadly offer two types: transformer isolation and transformerless PV inverters. Transformerless PV inverters hold promise for increased efficiency and reduced system cost. However, they are plagued by a common issue known as CM currents, which can negatively impact the overall system. To address this issue, researchers have focused on improving the suppression of the CM current in transformerless PV inverters. One approach involves employing a full bridge topology with four switches. However, this method comes with its own set of challenges. In particular, when using bipolar modulation in the full-bridge topology, there are inherent drawbacks such as increased losses and the presence of double inductance due to output voltage at the two-level bipolar. Additionally, researchers have explored alternative strategies focused on achieving galvanic isolation between the PV array and the grid within existing transformerless inverter topologies. For instance, the H5 topology introduces additional switches between the bridge arms and the input. This modification aims to mitigate the CM's current issues and enhance the overall reliability and performance of the PV inverter system.

## III. METHODOLOGY

The proposed methodology introduces two distinct operational modes for analyzing CM current in the context of H5 topology, focusing on the significance of switch junction capacitors. The first mode is "power transmission mode," which characterizes the switching behavior while transmitting the input power to the grid. The power transmission mode is illustrated in Figs. 1a and 1b based on the capacitor's charge and discharge. In the second operational mode, designated as "freewheeling mode," the inverter transitions to a state where power transfer from the input (PV array) to the grid ceases. During this interval, the current generated by the filter inductors continues to flow uninterruptedly into the grid network. This mode plays a crucial role in maintaining system stability and efficiency during specific switching conditions. This mode is depicted in Figs. 2a and 2b.Maintaining the Integrity of the Specifications.

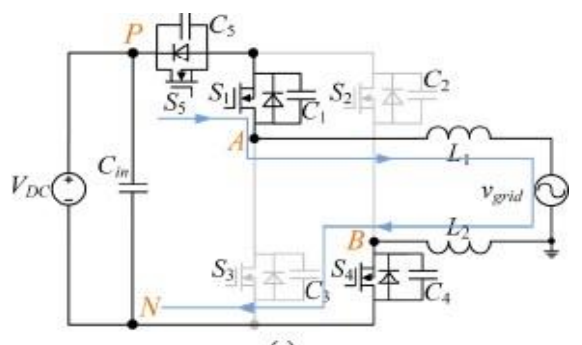


Fig. 1a Power Transmission Mode

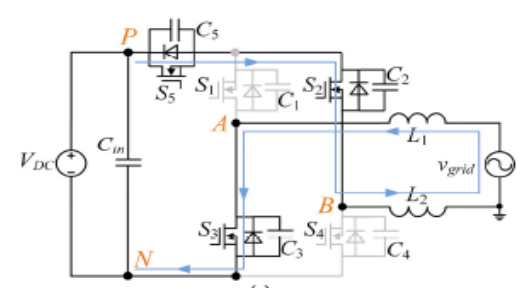


Fig. 1b Power Transmission mode

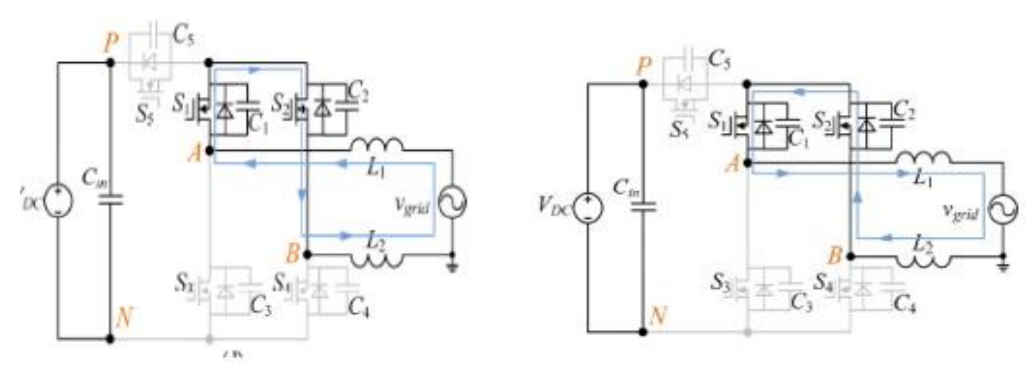


Fig. 2a Free Wheeling Mode

Fig. 2b Free Wheeling Mode

The analysis considers the time-varying nature of CM voltage due to inherent asymmetrical structure of the H5 topology, particularly concerning the discharging and charging processes of switch junction capacitors. During the positive half period of operation, the transition to freewheeling mode via power transmission mode is characterized by the synchronous deactivation of switches S4 and S5. Subsequently, capacitors C4 and C5 are charged while C2 and C3 are discharged. This initial phase establishes the voltage across each junction capacitor. After entering the freewheeling mode, facilitated by the conduction of switch S2, Kirchhoff's current law is applied at point A to analyze the circuit dynamics. However, it is crucial to acknowledge that the CM voltage in the H5 topology remains constant at VDC during the power transmission mode. This observation underscores the challenge of maintaining a constant CM voltage throughout the operational period, potentially leading to fluctuations in CM current. Consequently, achieving a constant CM voltage is paramount for effectively eliminating CM currents within the H5 topology.

Single-phase induction motors, while common, face inherent limitations during startup. Unlike their three-phase counterparts, which generate a rotating magnetic field, single-phase motors utilize a single winding, resulting in a pulsating field upon AC supply. This pulsating nature, instead of continuous rotation, prevents the motor from self-starting due to rotor inertia. The circuit parameters are tabulated in Table 1 using the various parameters are brake-drum circumference, that is, " $2\pi R$  (m)", where brake drum radius R = 0.082 m. This equation is derived from the formula for the circumference of a circle, where  $2\pi R$  represents the distance around the outer edge of the circular brake drum. The equation for Input power = "V I X cos  $\Phi$ " calculates the input power in watts (W). Here, voltage represents volts (V), current represents I in amperes (A), and phase angle is represented by  $\Phi$ , that is phase angle between the current and voltage. The term VI is the apparent power, and the power factor is cos $\Phi$ . The power factor directly reflects the ratio of real power (P) delivered to the load to the apparent power (S) drawn from the source.

The equation Torque (T) =  $9.81* R \times (S_1 \sim S_2)$  (N-m) calculates the torque in Newton-meters (*N-m*) tabulated in Table 1. Here, the radius is represented by *R* of the brake drum, and  $S_1$  and  $S_2$  represent the readings from the spring balance in kilograms (kg). The difference between  $S_1$  and  $S_2$  represents the change in force applied, which is then multiplied by the radius and gravity (9.81 m/s2) to calculate torque. For example,  $S_1 = 0.9.11$ , 12, 13, 14, 15;  $S_2 = 0.3.3.3$ , 3, 3, 3, 3 and N = 1492, 1464, 1449, 1428, 1412, 1402, 1397. The equation for output power =  $2\pi NT/60$  (watts) calculates the output power in watts (*W*) tabulated in Table 1 and 2. Here, *N* represents the speed in revolutions per minute (rpm), and *T* represents the torque in Newton-meters (*N-m*). This equation is derived from the relationship between power, torque, and rotational speed. The equation for % Efficiency ( $\eta$ ) = (output power/input power) \*100 calculates the efficiency of the system as a percentage tabulated in Table 1. The efficiency

of the system is evaluated by comparing the output power to the input power. A higher percentage obtained from this comparison signifies a greater efficiency in converting input power to usable output power.

Voltage V(volts)	Current I(Amps)	Torque T(Nm)	Output Power (W)	Power Factor (cosΦ)	Speed N(rpm)	Efficiency η (%)
220	7.6	4.2	115	0.62	659	85
210	7.5	4.1	110	0.62	650	88
200	7.4	4.1	105	0.62	629	86
180	7.1	4.0	98	0.62	620	82
170	7.1	4.0	96	0.62	615	80
160	7.0	3.9	94	0.62	610	78
150	7.0	3.8	92	0.62	600	76

Table. 1 PROPOSED SYSTEM

The equation for Power factor=cos  $\Phi$  calculates the power factor shown in Table 1 to measure of how effectively power is being transformed into suitable work. The power factor angle ( $\Phi$ ) typically ranges from 0° to 90°. In the context of operating at full load, when the motor exhibits a lagging power factor, which signifies an inductive load, the power factor angle would be between 0° and 90°. This means the current lags behind the voltage due to the inductive nature of the motor's windings. Conversely, In the scenario where the motor operates at full load while exhibiting a leading power factor (characteristic of capacitive behavior), the power factor angle would also be between 0° and 90°, indicating that the current leads the voltage. The specific range of  $\Phi$  during a load test will depend on the testing conditions and objectives. Engineers conducting the test may vary the load and monitor the power factor angle across different load conditions to assess the motor's performance and efficiency under various operating conditions.

The flowchart shown in FIG. 3 outlines the motor testing process, which is essential for ensuring the quality and efficiency of motors used in various mechanical systems. The process begins by initiating the motor testing procedure. In next step, the motor's specifications are thoroughly examined. These specifications include critical details such as voltage ratings, current requirements, and power output.

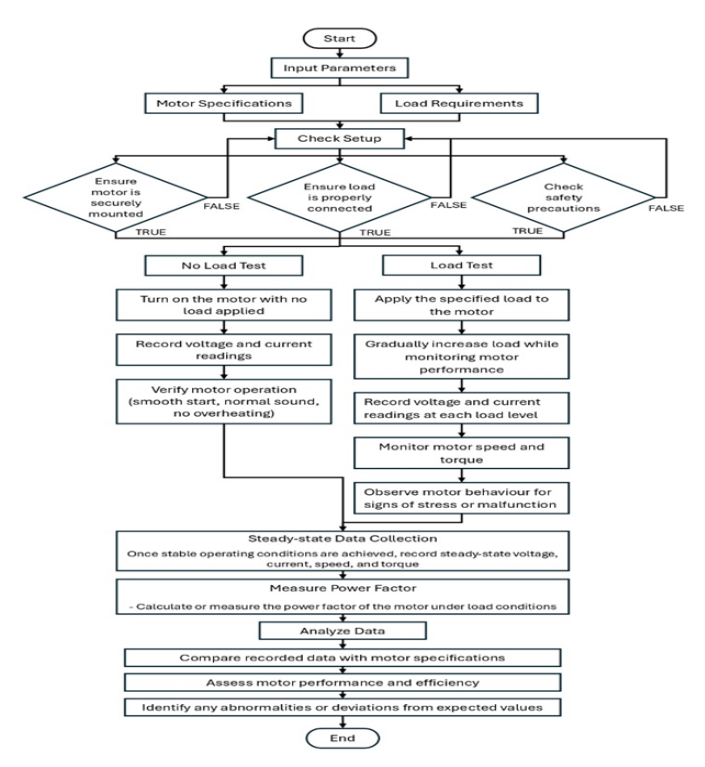


FIG. 3 Flow chat for identifying an analyzing the efficiency

By verifying these parameters, we ensure that the motor is suitable for the intended application. Thereafter, the motor is physically connected to appropriate testing equipment. This step allows us to measure and monitor the motor's performance accurately. Proper connections are essential for obtaining reliable data during testing. To simulate real-world conditions, a load is applied to the motor. This load represents the actual workload the motor will encounter in its operational environment. By subjecting the motor to this load, we assess its behavior under stress. Various parameters are measured during this phase: Speed: The motor's rotational speed (in revolutions per minute or RPM) is recorded; Torque, which represents the twisting force exerted by the motor, is measured; and The motor's efficiency (how effectively it converts electrical energy into mechanical work) is evaluated. The measured values are compared to the motor's specified parameters that helps to determine whether the motor meets the desired performance criteria. Based on the comparison in the previous step, a decision is made. If the motor's performance aligns with the specified parameters, it passes the test. Otherwise, it fails. A passing motor is considered suitable for use, while a failing motor may require adjustments or further investigation.

Enters the specifications of the motor being tested and specifies the load that will be applied to the motor during the testing process as shown in FIG. 4. Before starting the test, it's important to make sure that the motor is securely fastened to the test bench which will prevent the motor from moving or vibrating excessively during operation, which could lead to inaccurate test results or even damage the motor. Similarly, it's important to verify that the load is properly connected to the motor. A loose or improper connection could also lead to inaccurate test results or damage the motor. With the setup checks complete, the motor is turned on without any load applied. During the no-load test, the current readings of the motor and also voltage readings are recorded. During unloaded motor operation, visual and auditory inspection by the operator are essential to confirm proper functionality. This includes checking for a smooth start, normal sound, and no signs of overheating

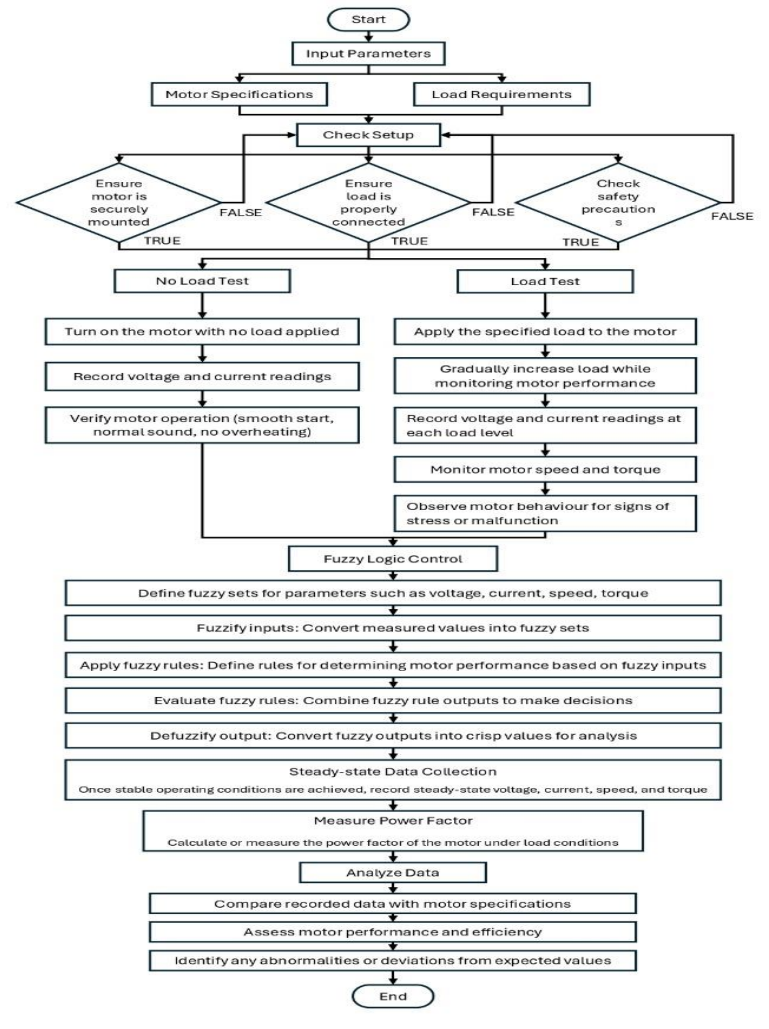


FIG. 4 Flowchat for idenfiying an analyzing the efficiency using fuzzy logic control

Once the no-load test is successful, the specified load is applied to the motor. The load should be applied gradually to avoid putting undue stress on the motor. With the load applied, the load is gradually increased while the motor's performance is closely monitored. Fuzzy logic control works by converting precise numerical values into fuzzy sets. The measured values from the motor test (voltage, current, speed, torque) are converted into fuzzy set memberships. This allows the fuzzy logic system to reason with these imprecise values. Apply the fuzzy rules to establish the association involving the fuzzy inputs and the desired motor performance. Then the fuzzy rules are evaluated established on the fuzzified inputs, and a fuzzy output is generated. This output represents the desired control action for the motor. Finally, the fuzzy output is converted back into a crisp numerical value that can be used to control the motor. After the motor reaches a stable operating state under the applied load, various data points are collected for analysis. The voltage, current, speed, and torque readings of the motor are recorded at this stable operating point. The power factor is a measure of how efficiently the motor is converting electrical energy into mechanical energy. The recorded data from the test is compared against the motor's specifications. This comparison helps to determine if the motor is performing within its expected range. By analyzing the collected data, the overall performance and efficiency of the motor under load can be assessed. Any deviations from the expected values or any abnormalities in the data can be identified at this stage. This information can be used to diagnose potential problems with the motor. As illustrated in Figure 5, the hardware configuration for the single-phase induction motor load test is presented in its entirety

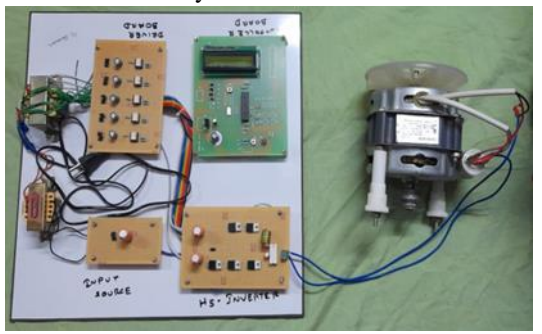


Fig.5 HARDWARE SETUP

## IV. RESULTS AND DISCUSSIONS

Simulation results demonstrate that the H5-D topology effectively suppresses CM current compared to its conventional counterpart. The addition of the clamping diode significantly reduces voltage fluctuations, thereby minimizing electromagnetic interference and emphasizes the specific context of the research, focusing on transformerless PV inverters. Experimental testing corroborates the simulation findings, affirming the superiority of the H5-D topology in mitigating CM current. The experimental results further highlight the practical feasibility and benefits of implementing the H5-D topology in real-world PV systems.

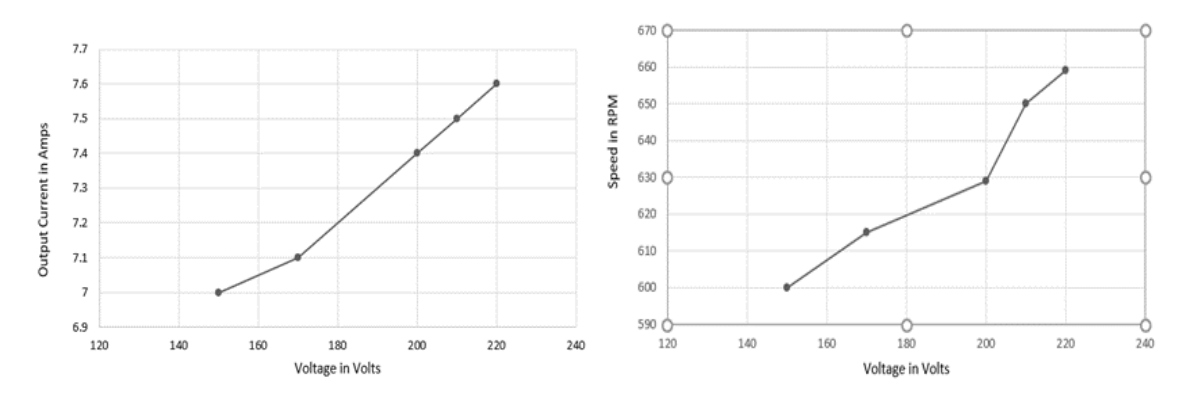


Fig. 6 Voltage Vs Output Current

Fig. 7 Voltage Vs Speed

Fig. 6 shows the linear relationship between volatge and output current. To provide an accurate analysis of the voltage vs. output current characteristics of an proposed system, the following specific information are to be considered to make the outline of the general approach for determining this relationship. Relationship between

variaion of voltage ans speed is shown in Fig. 7. Determining the voltage vs. speed relationship typically involves systems that use electric motors, such as those found in various applications like fans, pumps, or electric vehicles. Remember that the voltage vs. speed relationship of a motorized system is influenced by various factors including motor type, load conditions, and control mechanisms.

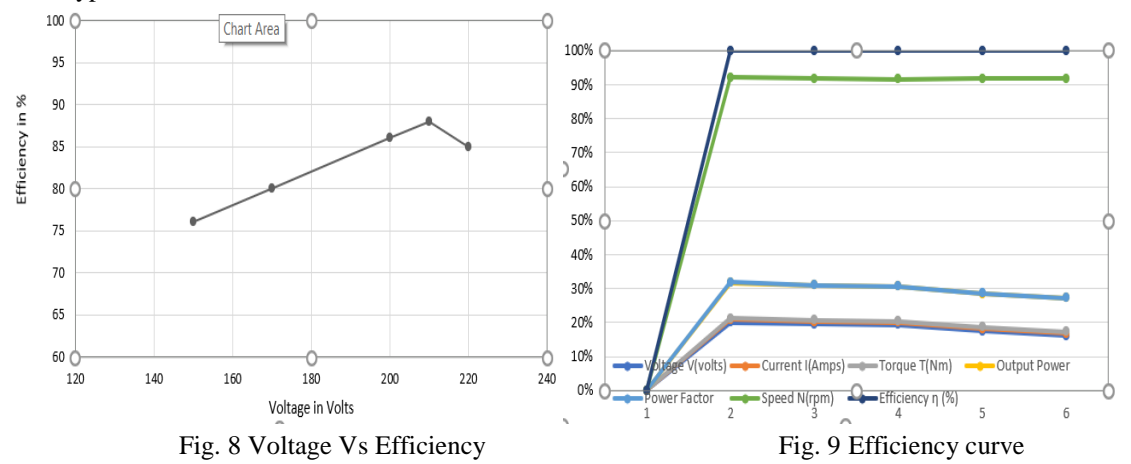


Fig. 8 shows the variation of efficiency with voltage. Determining the voltage vs. efficiency relationship of an existing system involves understanding how the efficiency of the system changes with variations in voltage. Remember that the voltage vs. efficiency relationship of a system can be influenced by various factors including component characteristics, operating conditions, and system design. Single-phase induction motor efficiency curve is shown in Fig. 9. Analysing the efficiency curve of a single-phase induction motor provides valuable insights into its performance characteristics across different load conditions. The following significant features are to be considered while conducting the load test. The efficiency curve of the motor plots the motor's efficiency against the load it is operating under. At a specific load level, the motor reaches its peak efficiency, where it converts electrical input power into mechanical output power most effectively. This point on the efficiency curve represents the optimal operating condition for the motor in terms of energy conversion efficiency. At light loads, the efficiency of a single-phase induction motor tends to decrease. This drop in efficiency is primarily due to factors such as increased winding losses, core losses, and friction losses relative to the reduced mechanical output power. Similarly, at heavy loads approaching the motor's rated capacity, the efficiency may decrease as well. This decrease is often attributed to factors such as increased copper losses in the windings and higher mechanical losses due to friction and windage. Beyond the motor's rated load, the efficiency curve typically exhibits a steeper decline. Operating the motor beyond its rated capacity can lead to excessive heating, reduced efficiency, and potential damage to the motor due to overloading. Selecting an operating point on the efficiency curve that aligns with the motor's peak efficiency is crucial for maximizing energy efficiency and minimizing operating costs. Designing systems with appropriate load matching and control mechanisms can help achieve this optimal operating point. The specific shape and characteristics of the efficiency curve can vary depending on factors such as motor design, size, construction materials, and manufacturing quality. The Fuzzy Inference System (FIS) utilizes a rule base to arrive at a conclusion based on the processed input variables. This process entails converting the input variables into corresponding linguistic variables that the FIS can understand. Figure 10-12 depicts the membership functions employed for the input variables, output variable, and control signals within the FIS.

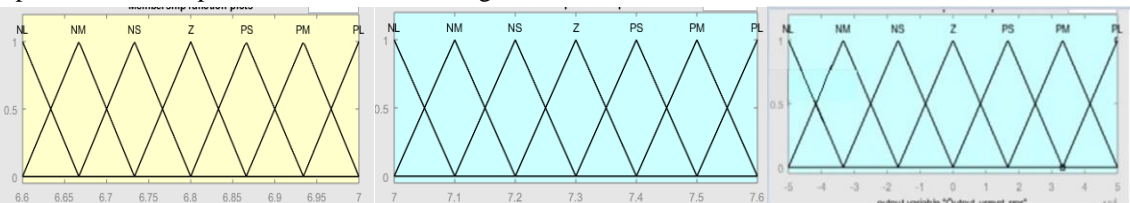


Fig. 10 FIS of (a) output current I; (b) input current; (c) output current error

Fig. 11 Fuzzy logic design for (a) AV; (b) Input variable 'error'; (c) Input variable 'integral of error'

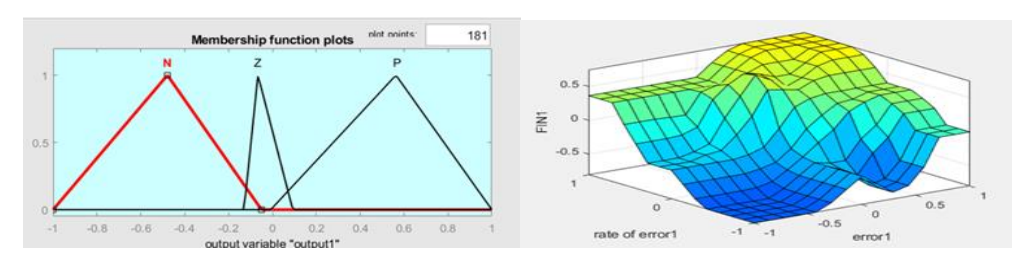


Fig. 12 Fuzzy membership functions of (a) output variable; (b) Surface diagaram

Fig. 12 (b) shows the surface diagram of Fuzzy inference system. A surface diagram in the context of a fuzzy inference system typically refers to the representation of the fuzzy inference process in a three-dimensional space, illustrating how input variables are mapped to output variables through fuzzy logic rules. This visualization helps in understanding the behaviour of the system and the relationship between inputs and outputs. The axes of the surface diagram represent the input variables of the fuzzy inference system. Each axis corresponds to one input variable, and the range of each axis spans the possible values of that variable. For example, if the fuzzy inference system has two input variables, "Temperature" and "Humidity," the surface diagram would have two axes labelled accordingly. The surface of the diagram represents the output variable of the fuzzy inference system. The surface contours or colours depict the fuzzy output values corresponding to different combinations of input variables. The range of the output variable is typically represented along the vertical axis or through colour gradients on the surface. The surface diagram may include visual representations of the membership functions associated with each input variable. These functions determine how input values are fuzzified into linguistic terms. The shapes and characteristics of the membership functions influence the shape of the output surface. Each fuzzy IF-THEN rule in the rule base contributes to a rule surface in the diagram. A rule surface defines the relationship between input variables and the consequent (output) variable for a specific rule. The intersections of these rule surfaces create a complex surface that represents the overall behaviour of the fuzzy inference system. Analysts can interpret the surface diagram to understand how changes in input variables affect the output variable. By observing the contours or gradients on the surface, one can identify regions of high or low output values and assess how sensitive the system is to variations in input variables. Surface diagrams can be used for system optimization and analysis. Engineers can adjust membership functions, rule base, or input variable ranges to optimize system performance or to address specific requirements. Various software tools and programming libraries can be used to create surface diagrams for fuzzy inference systems. These tools allow for interactive exploration of the system's behaviour and facilitate model development and validation. Overall, a surface diagram provides an intuitive and visual representation of the fuzzy inference process, and effective information decisions regarding system design and operation.

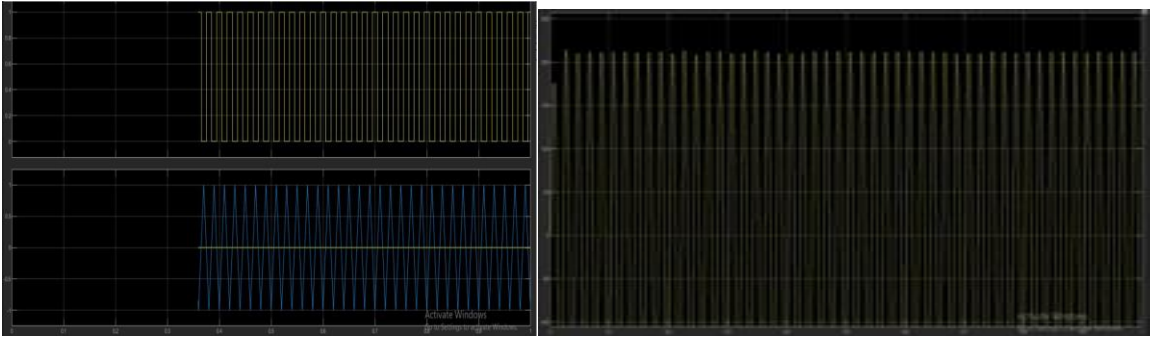
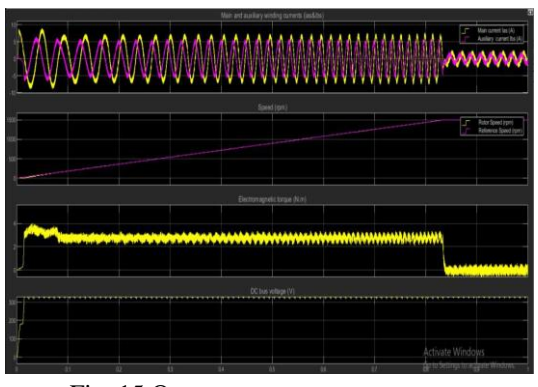


Fig. 13 Pulse Generation

Fig. 14 DC Output



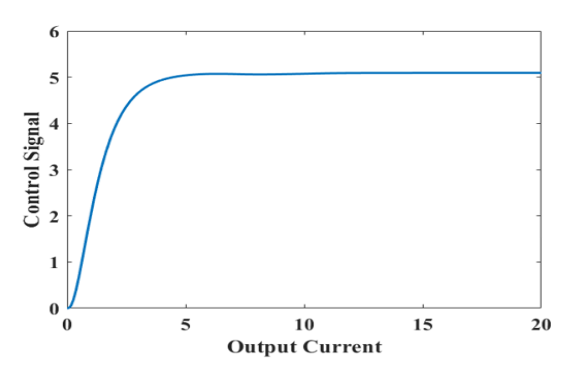


Fig. 15 Output

Fig. 16 Output current Vs control signals.

By analyzing and modeling the performance of photovoltaic grid-connected H5 inverters, the system can be optimized for maximum efficiency, reliability, and stability. AI techniques leading to better optimization. By analyzing data from load tests on induction motors, AI algorithms can identify early signs of degradation or malfunction and alert maintenance teams before major issues arise. AI techniques can facilitate intelligent energy management strategies, such as demand-side management and load balancing. By analyzing data from load tests and modeling system performance, AI can optimize energy usage and distribution, leading to cost savings and improved grid stability. By leveraging AI techniques for fault detection and predictive maintenance, the reliability of the photovoltaic grid-connected H5 inverter system can be significantly enhanced. This can lead to improved uptime and reduced risk of unexpected failures, ensuring continuous power supply to critical loads. Photovoltaic grid-connected systems often operate under dynamic and variable conditions, such as changes in weather and load demand. AI-based modeling and analysis can adapt to these changing conditions in real-time, optimizing system operation and maximizing energy production. Research and development in the field of photovoltaic grid-connected systems, combined with AI techniques, can drive technological innovation. New algorithms and methodologies developed through this research can lead to advancements in renewable energy integration and grid management.

# V. CONCLUSION AND FUTURE SCOPE

This paper presents the H5-D topology, a novel transformerless photovoltaic (PV) inverter configuration specifically designed to achieve superior common-mode (CM) current suppression. The proposed H5-D topology leverages a simple and practical design, employing only five switches and a single diode, making it well-suited for single-phase PV inverter applications. Furthermore, a meticulously crafted modulation strategy is incorporated within the H5-D topology. This strategy ensures that the inverter's CM voltage remains constant throughout operation. Consequently, the resulting CM currents are demonstrably reduced to approximately one-third of those observed in the conventional H5 topology, under identical electrical parameters and utilizing the same power switches. The effectiveness of the H5-D topology is corroborated through both simulation and experimental validation, solidifying the theoretical underpinnings presented in this work. The H5-D topology's inherent simplicity and practicality render it particularly advantageous for single-phase transformerless PV inverter systems. Significantly, the H5-D topology maintains a constant CM voltage, effectively mitigating ground leakage currents. Additionally, it exhibits a differential mode characteristic comparable to a unipolar modulation H4 inverter, achieving this without incurring any losses within the supplementary clamping diode branch. This translates to superior efficiency and the ability to function with a low-input voltage requirement similar to the H4 inverter. Experimental investigations have demonstrably validated the viability and efficacy of the proposed H5-D topology in real-world applications

VI. COPYRIGHT FORMS AND REPRINT ORDERS

COPYRIGHT DECLARATION Journal of Electrical Systems (JES)

Title of the Article: ANALYZING PHOTOVOLTAIC GRID-CONNECTED H5 INVERTER WITH ARTIFICIAL INTELLIGENCE FOR INDUCTION MOTOR LOAD TESTING AND EVALUATION

#### Authors.B.RAJAPANDIAN, G.T.SUNDARRAJAN

I/We hereby assign copyright of the article named above (the Work), to the publisher, Journal of Electrical Systems (JES). I/We understand that Journal of Electrical Systems (JES) will act on my/our behalf to publish, reproduce, distribute and transmit the Work and will authorize other reputable third parties (such as document delivery services) to do the same. I/We warrant that the Work has not been published before in its current or a substantially similar form and is not under consideration for another publication, does not contain any unlawful statements. I/We warrant that "proof of consent" has been obtained for studies of named organizations and people. All authors have received a final version of the Work, take responsibility for the content and agree to its submission. I/We assert my/our moral rights to be identified as the author/s of the Work.

1. Signature

Author Name B. RAJAPANDIAN

2. Signature Date 19.9.2024 Place CHENNAI

Author Name G.T. SUNDARRAJAN

Date 19.9.2024 Place CHENNAI

#### ACKNOWLEDGMENT

First and foremost, I would like to express my deepest gratitude to Sathyabama Institute of Science And Technology for providing me with the opportunity and the resources necessary to complete my Research works. The unwavering support, intellectual environment, and world-class facilities available at the institution have been instrumental in shaping the progress of this research.

I extend my sincere appreciation to Dr.G.T.Sundarajan whose guidance, mentorship, and expertise have been invaluable throughout the research process. Your insightful feedback and encouragement pushed me to pursue excellence at every stage and for your constructive criticism, thoughtful recommendations, and continuous encouragement. Your input has enriched this work immensely.

Special thanks to Department of Electrical and Electronics Engineering for fostering a collaborative and innovative research atmosphere in both Simulation laboratory and Power Electronics Laboratory.

### REFERENCES

- [1] R. González, J. López, P. Sanchis and L. Marroyo, "Transformer less inverter for single-phase photovoltaic systems," IEEE Trans. Power Electron., vol. 22, no. 2, pp. 693-697, Mar. 2007.
- [2] R. González, E. Gubía, J. López and L. Marroyo, "Transformer less single phase multilevel-based photovoltaic inverter," IEEE Trans. Ind. Electron., vol. 55, no. 7, pp. 2694-2702, Jul. 2008.
- [3] H. Jedtberg, A. Pigazo, M. Liserre, and G. Buticchi, "Analysis of the robustness of transformerless PV inverter topologies to the choice of power devices," IEEE Trans. Power Electron. vol. 32, no.7, pp. 5248-5257, Jul. 2017.
- [4] R. R. de Lima, F. C. Melo, L. S. Garcia, E. A. A Coelho, V. J. Farias and L. C. G. Freitas, "Design and modeling of a transformer less hybrid inverter system using a fuel cell as energy storage element for microgrids with sensitive loads," Proc. IEEE 6th Int. Symposium on Power Electron. for Distributed Generation Sys. Aachen, Germany, Jun. 2015, pp. 1-8.
- [5] H. Xiao and S. Xie, "Leakage current analytical model and application in single phase transformerless photovoltaic grid-connected inverter," IEEE Trans. Electromagnetic Compatibility, vol. 52, no. 4, pp. 902-913, Nov. 2010.
- [6] Z. Tir, O. P. Malik, and A. M. Eltamaly, "Fuzzy logic-based speed control of indirect field oriented controlled double star induction motors connected in parallel to a single six-phase inverter supply," Electr. Power Syst. Res., vol. 134, pp. 126– 133, May 2016. 57
- [7] J. A. Ali, M. A. Hannan, A. Mohamed, and M. G. M. Abdolrasol, "Fuzzy logic speed controller optimization approach for induction motor drive using backtracking search algorithm," Measurement, vol. 78, pp. 49–62, Jan. 2016
- [8] S. M. Gadoue, D. Giaouris, and J. W. Finch, "MRAS sensor less vector control of an induction motor using new sliding-mode and fuzzy-logic adaptation mechanisms," IEEE Trans. Energy Convers., vol. 25, no. 2, pp. 394–402, Jun. 2010 [9] S. V. Araújo, P. Zacharias and R. Mallwitz, "Highly efficient single phase transformer less inverters for grid-connected photovoltaic systems," IEEE Trans. Ind.

- [9] W. Cui, B. Yang, Y. Zhao, W. Li and X. He, "A novel single-phase transformer less grid-connected inverter," Proc. 37th Annu. Conf. IEEE Ind. Electron. Soc., Melbourne, VIC, Nov. 2011, pp. 1126-1130. Electron., vol. 57, no. 9, pp. 3118-3128, Sept. 2010.
- [10] Multi-Way Switching System Using IoT Premalatha, S., Kumar, T.S., Srividya, K., Rajapandian, B., Maadhavan, H.Proceedings of the 2021 4th International Conference on Computing and Communications Technologies, ICCCT 2021, 2021, pp. 215–218
- [11] B.Rajapandian, G.T.Sundarrajan, "Evaluation of DC-DC Converter using Renewable Energy Sources", International Journal of Power Electronics and Drives Systems (IJPEDS) Vol 11, No. 4December 2020, pp. 1918~1925
- [12] B.Rajapandian, K. Madhanamohan, T. Tamilselvi, R.Prithiga," Smart Dustbin", International Journal of Engineering and Advanced Technology (IJEAT) ISSN: 2249 8958, Volume-8, Issue-6, August 2019
- [13] T. Tamilselvi1, K. Kayalvizhi, B. Rajapandian, N.NithyaRani" A Research on Electronic Component Wrecker Using Electro-Magnetic Pulse (EMP)", International Journal of Engineering and Advanced Technology (IJEAT)ISSN: 2249 – 8958, Volume-8, Issue-6, August 2019
- [14] Rajapandian B, Harini V, Raksha D, Sangeetha V," A NOVEL APPROACH AS AN AID FOR BLIND, DEAF AND DUMB PEOPLE", 2017 IEEE 3rd International Conference on Sensing, Signal Processing and Security (ICSSS)
- [15] G. T. Sundar Rajan, "Power Quality Improvement at Input and Output Stages of Three Phase Diode Rectifier using Artificial Intelligent Techniques for DC and AC Drive Applications", IEEE International Conference on Computational Intelligence and Computing Research (ICCIC 2014, 2014), PARK College of Engineering and Technology, Coimbatore, Tamilnadu, INDIA, pp. 904 909, December 18 to 20. 978-1-4799-3972-5/14.